SCALING BEHAVIOR OF STRUCTURE FUNCTIONS OF THE LONGITUDINAL MAGNETIC FIELD IN ACTIVE REGIONS ON THE SUN

Abramenko, V.I.[1], **Yurchyshyn, V.B.**[1,2],
Wang H.[2], **Spirock, T. J.**[2], **Goode, P. R.**[2]

(1) *Crimean Astrophysical Observatory, 98409 Nauchny, Crimea, Ukraine*

(2) *Big Bear Solar Observatory, 40386 North Shore Lane, Big Bear City, CA 92314, USA*

In the framework of a refined Kolmogorov's hypotheses, the scaling behavior of the B_Z–component of the photospheric magnetic field is analyzed and compared to flaring activity in solar active regions. We used SOHO/MDI, Huairou (China) and Big Bear measurements of the B_z-component in the photosphere for nine active regions. We show that there is no universal behavior in the scaling of the B_z-structure functions for different active regions.

Our previous study has shown that scaling for a given active region is caused by intermittency in the field, $\varepsilon^{(B)}(\vec{x})$, describing the magnetic energy dissipation. When intermittency is weak, the B_z-field behaves as a passive scalar in the turbulent flow and the energy dissipation is largely determined by the dissipation of kinetic energy in the active regions with low flare productivity. However, when the field $\varepsilon^{(B)}(\vec{x})$ is highly intermittent, the structure functions behave as transverse structure functions of a fully developed turbulent vector field and the scaling of the energy dissipation is mostly determined by the dissipation of the magnetic energy (active regions with strong flaring productivity).

Based on this recent result, we found that the dissipation spectrum of the B_z component is strongly related to the level of flare productivity in a solar active region. When the flare productivity is high, the corresponding spectrum is less steep. We also found that during the evolution of NOAA AR 9393, the B_z dissipation spectrum becomes less steep as the active region's flare activity increases. Our results suggest that the reorganization of the magnetic field at small-scales is also relevant to flaring: the relative fraction of small-scale fluctuations of magnetic energy dissipation increases as an active region becomes prone to produce strong flares.

Since these small scale changes seem to begin long before the start of a solar flare, we suggest that the relation between scaling exponents, calculated by using only measurements of the B_z component, and flare productivity of an active region may be used to monitor and forecast flare activity.

1. Introduction

The flow of a highly nonlinear system is complex, giving rise to vortices at different scales. Such flows are called turbulent. Small-scale vortices acquire energy as a result of the breakdown of large-scale vortices. This sets up a cascade of energy transfer to smaller and smaller scales. The process is believed to stop at the smallest scale where the energy is dissipated into heat.

The solar plasma, that transports embedded magnetic fields in the solar convective zone and in the photosphere, is also found to be in a turbulent state, which is characterized by a high magnetic Reynolds number (in the photosphere it is about 10^8, see, e.g. Zeldovich and Ruzmaikin 1987). Turbulence in the solar plasma is deeply tied to the generation and transfer of the magnetic field in the sun (Parker 1979; Petrovay and Szakaly 1993; Cataneo 1999) and on the solar surface (Seehafer 1994; Cadavid et al. 1999). It is now accepted that a solar flare draws its energy from the magnetic field. Therefore, it is natural to expect certain relationships between the parameters of turbulence of the magnetic field on the one hand and the parameters of magnetic energy dissipation and flaring capability on the other. The present study is devoted to the examination of this expectation.

2. Method

Since Kolmogorov's study (1941), many models have been proposed to describe the statistical behavior of fully developed turbulence. In these studies, the flow is modeled using statistically averaged quantities, such as velocities, and structure functions play significant roles. Structure functions, which are equivalent to the correlation function of fluctuation velocities between two different spatial points, were first introduced by Kolmogorov (1941) and they are defined as statistical moments of the field increments:

$$S_q(r) = \langle |\mathbf{u}(\mathbf{x}+\mathbf{r}) - \mathbf{u}(\mathbf{x})|^q \rangle, \tag{1}$$

where $\mathbf{r}$ is a separation vector, and q is a real number. Structure functions, calculated within the inertial range of scales, r, ($\eta \leq r \leq L$, where η is a spatial scale where the influence of viscosity becomes significant and L is a scaling factor for the whole system) are described by the power law (Kolmogorov 1941; Monin and Yaglom 1975):

$$S_q(r) \sim (\varepsilon_r(\mathbf{x}) \cdot r)^{q/3} \sim (r)^{\zeta(q)}. \tag{2}$$

where $\varepsilon_r(\mathbf{x})$ is the energy dissipation, averaged over a sphere of size r (Monin and Yaglom 1975).

The function $\zeta(q)$ describes one of the most important characteristics of a turbulent field. In order to estimate this function, Kolmogorov (1941, hereinafter as K41) assumed, that for fully developed turbulence (turbulence at high Reynolds number), the probability distribution laws of velocity increments depend only on the first moment (mean value), $\bar{\varepsilon}$, of the function $\varepsilon_r(\mathbf{x})$. Replacing $\varepsilon_r(\mathbf{x})$ in equation (2) by $\bar{\varepsilon}$ we have:

$$S_q(r) \sim (\bar{\varepsilon} \cdot r)^{q/3} = C \cdot r^{q/3}, \tag{3}$$

where C is a constant. As a result, function $\zeta(q)$ is defined as a straight line with a slope of $1/3$:

$$\zeta(q) = q/3. \tag{4}$$

Kolmogorov further realized that such an assumption is very rigid and turbulent state is not homogeneous across spatial scales. There is a greater spatial concentration of turbulent activity at smaller scales than at larger scales. This indicates that the energy flow and dissipation do not occur everywhere, and that the energy dissipation field should be highly inhomogeneous (intermittent) and also follow a power law,

$$\langle(\varepsilon_r(\mathbf{x})^p\rangle \sim r^{\tau(p)}, \tag{5}$$

where p is a real number. Then equation (2) may be rewritten as

$$S_q(r) \sim (\varepsilon_r(\mathbf{x}) \cdot r)^{q/3} = (\varepsilon_r(\mathbf{x}))^{q/3} \cdot r^{q/3} = r^{\tau(q/3)} \cdot r^{q/3} \tag{6}$$

or

$$\zeta(q) = \tau(q/3) + q/3. \tag{7}$$

Equation (7) is now referred to as the refined Kolmogorov's theory (heretoforward, refined K41) of fully developed turbulence (Kolmogorov 1962a; Kolmogorov 1962b; Monin and Yaglom 1975; Frisch 1995).

One can see from equation (7) that the function $\zeta(q)$ deviates from a straight $q/3$ line. It has been suggested that the deviation is caused by the scaling properties of a field of kinetic energy dissipation. Equation (7) for velocity increments has been carefully checked many times over the last four decades and experimental results thus confirmed this suggestion (see Gurvich et al. 1963; Anselmet et al. 1984; Schmitt et al. 1994; Frisch 1995 and references in). In Figure 1a we reproduce a result published in Schmitt et al. (1994). One sees that $\zeta(q)$ is an increasing concave outward function crossing the K41 line at $q = 3$, where $\zeta(3) = 1$, which satisfies both K41 and refined K41 theories as long as $\langle(\varepsilon_r(\mathbf{x})^{3/3}\rangle = \bar{\varepsilon}$ (Monin and Yaglom 1975).

We would like to note that very important information on a turbulent field can be derived from structure functions $\zeta(q)$, which can be, in principle, obtained from experimental

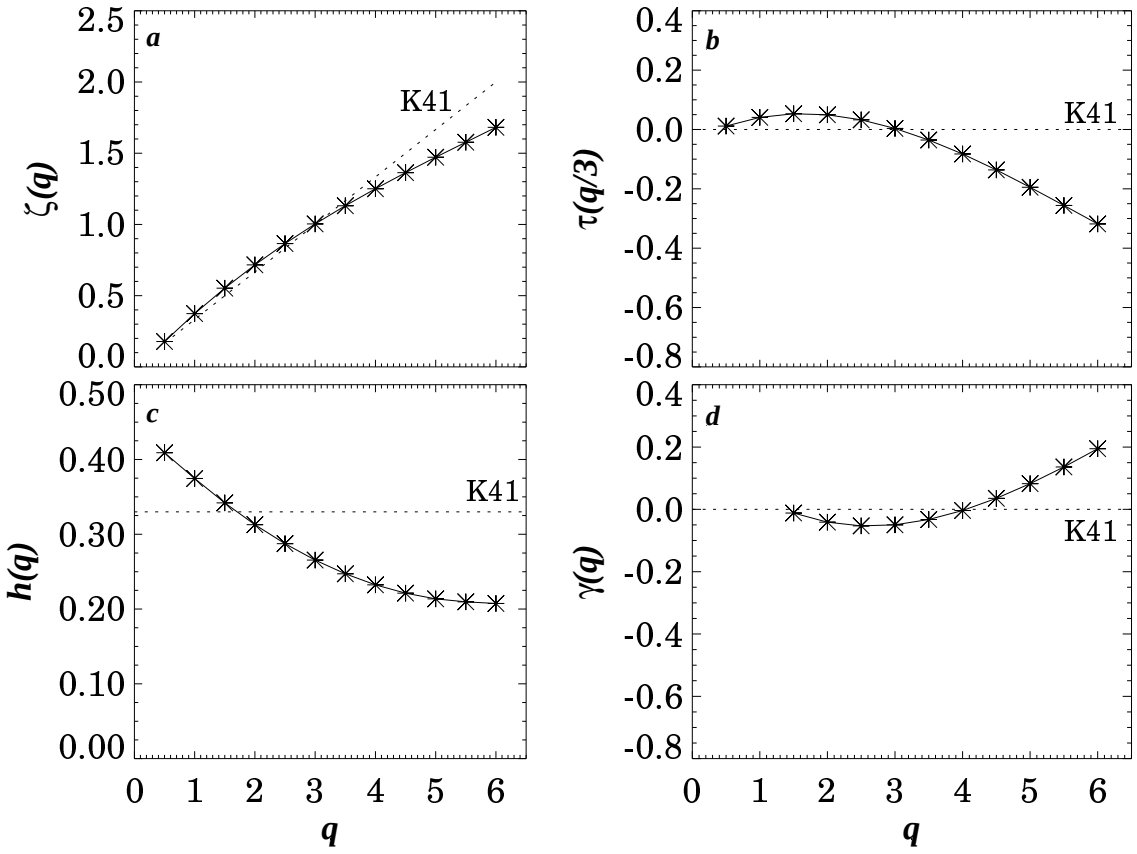

Fig. 1.— Parameters of fully developed turbulence calculated using structure functions defined from measurements of wind velocities in the earth's atmosphere. *(a)* - exponents $\zeta(q)$ of structure functions are shown as a function of order q (experimental data from Schmitt et al., 1994); *(b)* - scaling exponents $\tau(q/3)$ of the kinetic energy dissipation field calculated by using (7); *(c)* - plot of the derivative $h(q)$ of function $\zeta(q)$ calculated by using (10). Panel *(d)* shows function $\gamma(q)$ that is a correction term to $q/3$ in equation (11). The dotted line K41 shows the Kolmogorov's straight line - the behavior of all parameters in frame of the classical Kolmogorov's K41 theory of fully developed turbulence.

data. For example, the value of the function at $q = 6$ deserves special attention because it defines a power index

$$\beta \equiv 1 - \zeta(6) \tag{8}$$

of a spectrum $E^{(\varepsilon)}(k)$ of energy dissipation $\varepsilon(\mathbf{x})$ that is given by (Monin and Yaglom 1975):

$$E^{(\varepsilon)}(k) \sim k^{\beta}, \tag{9}$$

where k is a wave number. Observed values β for a velocity field at fully developed turbulence were found to be in the range of $-0.8 \leq \beta \leq -0.6$ (Gurvich et al. 1963; Anselmet et al. 1984).

Having $\zeta(q)$, derived from experimental data, and by using equation (7) one can calculate the scaling exponent $\tau(q/3)$ in equation (5) for the energy dissipation field. For example, in Figure 1b we show function $\tau(q/3)$ calculated for a velocity field at fully developed turbulence by using function $\zeta(q)$ shown in Figure 1a. The scaling exponent $\tau(q/3)$ is a concave function, which equals zero at $q = 3$ and $\tau(q/3) \approx -0.33$ at $q = 6$, which gives power index $\beta = -0.67$.

The derivative of $\zeta(q)$,

$$h(q) \equiv \frac{\mathrm{d}\zeta(q)}{\mathrm{d}q}, \tag{10}$$

can also be obtained by using the $\zeta(q)$ function (Figure 1c). The deviation of $h(q)$ from a constant value is a direct manifestation of *intermittency* in a turbulence field, which is equivalent to the term *multifractality* in fractal terminology (Frisch 1995; Feder 1988).

According to fractal theory, an intermittent structure consists of subsets, each of which follows its own scaling law. In other words, all values of h, within some range, are permitted and for each value of h there is a fractal set with an h-dependent dimension $D(h)$ near which scaling holds with exponent h. (Frisch 1995). In the framework of turbulence theory (Monin and Yaglom 1975; Zeldovich et al. 1987), the term *intermittency* is usually referred to as the ability of small-scale turbulent features to concentrate into high intensity separate blobs (tubes or sheets) surrounded by extend areas of much lower oscillations. Physically, these two treatments of *intermittency* are equivalent to each other (Frisch 1995).

Equation (7) may become even more complicated when we consider structure functions calculated for a chaotic field of passive scalar B transported by a turbulent flow. Under an assumption that fluctuations in the energy dissipation of a passive scalar and that of a velocity field are statistically independent, Abramenko (2002) obtained an equation which defines scaling of a passive scalar as

$$\zeta(q) = q/3 + \tau^{(B)}(q-1) - \tau^{(v)}((q-1)/3) \equiv q/3 + \gamma(q). \tag{11}$$

Here, $\tau^{(B)}(q)$ and $\tau^{(v)}(q)$ are scaling exponents of fields of energy dissipation $\varepsilon_r^{(B)}$ of a passive scalar, B, and of kinetic energy dissipation $\varepsilon_r^{(v)}$, respectively. In this case, the scaling exponents are defined as

$$\langle (\varepsilon_r^{(B)})^q \rangle \sim r^{\tau^{(B)}(q)}, \quad \langle (\varepsilon_r^{(v)})^q \rangle \sim r^{\tau^{(v)}(q)}. \tag{12}$$

Scaling exponents $\tau^{(B)}$ and $\tau^{(v)}$ in equation (11) have opposite signs. Therefore, the degrees of intermittency in the fields $\varepsilon_r^{(B)}(\mathbf{x})$ and $\varepsilon_r^{(v)}(\mathbf{x})$ compete in producing scaling of a passive scalar. Now, function $\zeta(q)$ may not satisfy the condition $\zeta(3) = 1$, and it may not necessarily be concave.

Let us consider two extreme cases in the behavior of function $\zeta(q)$ that are of particular interest.

1. In the case of a weakly intermittent field with the energy dissipation of a passive scalar,

$$|\tau^{(v)}((q-1)/3)| \gg |\tau^{(B)}(q-1)| \approx 0 \tag{13}$$

and function $\gamma(q)$ in equation (11) is determined mainly by scaling of kinetic energy dissipation

$$\gamma(q) \approx -\tau^{(v)}((q-1)/3). \tag{14}$$

Then, the scaling of a passive scalar is defined by kinetic energy dissipation and the function $\gamma(q)$ (see Figure 1d) is equivalent to function $\tau(q/3)$ that was mirrored relative to a horizontal line $y = 0$ and shifted to the right along the q axis.

2. In the case of a highly intermittent field with the energy dissipation of a passive scalar

$$|\tau^{(B)}(q-1)| \gg |\tau^{(v)}((q-1)/3)| \tag{15}$$

and both functions $\gamma(q)$ and $\zeta(q)$ in equation (11) are mostly defined by the intermittency of the passive scalar energy dissipation. As negative term $\tau^{(v)}((q-1)/3)$ in equation (11) becomes negligible, then the function $\gamma(q)$ becomes similar to $\tau(q/3)$ (Figure 1b). In this case, the scaling behavior of a passive scalar is rather similar to that of vector field.

For turbulence at large magnetic Reynolds numbers within the inertial range separations, the B_z-component of the magnetic field diffuse in exactly the same way as a scalar field (see, for example, Parker 1979; Petrovay and Szakaly 1993). Therefore, we can apply the above equations to investigate scaling of a passive scalar in order to understand structure functions of the B_z-component of the magnetic field calculated for an active region magnetogram.

Near the center of the solar disk the projection effect is negligible. Therefore, measurements of the longitudinal magnetic field represent the vertical component, B_z, of the magnetic field. We will define a coordinate system (x, y, z), where the (x, y) plane is tangential to the solar surface. Thus, the field B_z is the vertical component of the magnetic field $\mathbf{B}$, and it is defined on a grid

$$\omega : (x_i = i \cdot \Delta x, i = 1, ..., N_x; y_j = j \cdot \Delta y, j = 1, ..., N_y), \tag{16}$$

where Δx and Δy are the size of a grid cell measured in arc seconds, and N_x and N_y are the size of a magnetogram. Based upon the definition by Monin and Yaglom (1975), one can calculate a structure function of a field B_z:

$$S_q(r) = \langle |B_z(\mathbf{x} + \mathbf{r}) - B_z(\mathbf{x})|^q \rangle, \tag{17}$$

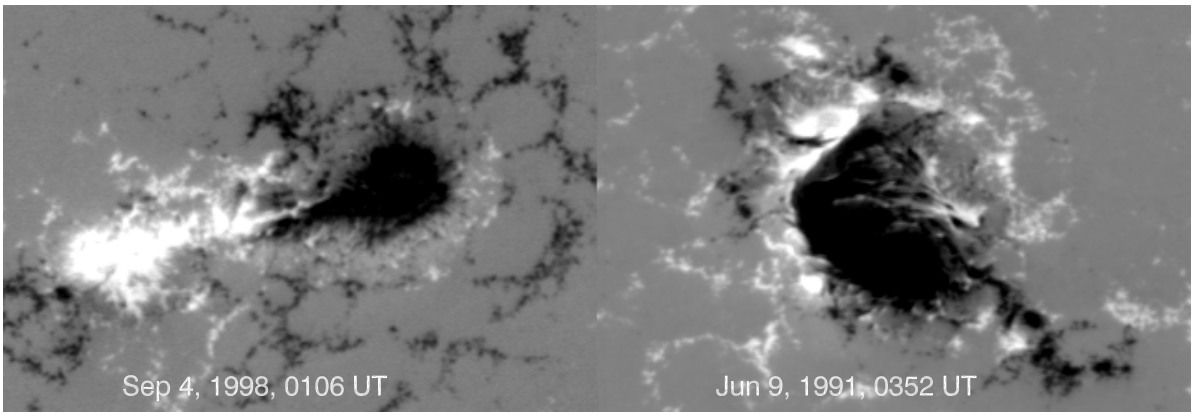

Fig. 2.— HSOS magnetograms for two active regions: *left panel* — NOAA AR 8323 magnetogram recorded on Sept 4, 1998 at 01:06 UT; *right panel* — NOAA AR 6659 magnetogram recorded on June 9, 1991 at 03:52 UT. North to the top, west to the right.

where $\mathbf{x} \in \omega$ and $r \equiv |\mathbf{r}|$ are real numbers between $r_{min} = 2\sqrt{\Delta x^2 + \Delta y^2}$ and $r_{max} < \min(N_x \cdot \Delta x, N_y \cdot \Delta y)$.

We would like to emphasize here that, according to the definition of Monin and Yaglom (1975), the transverse structure function $S_q^{(N)}(r)$ of a 3D vector field $\mathbf{B}$ is defined as

$$S_q^{(N)}(r) = \langle |B_z(\mathbf{x} + \mathbf{r}) - B_z(\mathbf{x})|^q \rangle. \tag{18}$$

The right sides in equations (17) and (18) are identical. Therefore, the scaling of the B_z-component reveals itself either as scaling as a passive scalar, or as scaling a 3D vector field.

3. Calculations of structure functions for eight active regions with different level of flaring activity

We selected data for eight active regions for which we will calculate parameters of turbulence of the photospheric magnetic field. Table 1 lists the active regions, their location on the solar disk as well as the date and time when a magnetogram was obtained. The data set includes one longitudinal magnetogram per active region (see examples in Figure 2). Magnetograms for all active regions except NOAA AR 8375 have been obtained with the videomagnetograph at Huairou Solar Observing Station (HSOS) of the National Astronomical Observatories of China (Wang et al. 1996). The data are measurements of the longitudinal magnetic field using the Fe I 5324Å spectral line and the pixel size is $0.62'' \times 0.43''$ (see Yurchyshyn et al. 2000). We also used one SOHO/MDI magnetogram

(Scherrer et al. 1995), which uses the Ni I 6767Å spectral line with a pixel size of $0.6'' \times 0.6''$, for active region NOAA 8375 .

Table 1: List of active regions

NOAA AR	Date	Time, UT	Coord.	Seeing
8375	Nov 4, 1998	16:32	N18 W08	10.0
8323	Sep 4, 1998	01:06	S16 W03	6.0
7216	Jul 4, 1992	00:29	N12 E12	6.0
7590	Oct 2, 1993	04:12	N13 E18	5.5
6786	Aug 20, 1991	02:19	S10 E04	5.5
6757	Aug 4, 1991	06:28	N18 W09	6.5
6850	Oct 3, 1991	03:21	S16 W20	7.0
6659	Jun 9, 1991	03:52	N29 W08	6.0

We established two requirements to select the data used in this study. The first requirement is that an active region should be located near the center of the solar disk where the measured longitudinal magnetic field represents the vertical component of an active region's magnetic field. The second requirement is that the data were obtained under satisfactory seeing conditions. In the 5th column of Table 1, we show the observer's estimation of the image quality on a scale of 1 to 10, where the SOHO/MDI magnetogram has an image quality of 10. On average, the HSOS data is a 2 - 3 in that scale with the maximum 7. In this paper, we used HSOS data with the image quality of 5.5, or better.

Using equation (17) we computed the structure functions $S_{q_i}(r)$ for different values of q_i, ranging from 0.5 up to 6.0, with an increment of 0.5. Each structure function $S_q(r)$ was calculated for 150 different spacial scales, r. Each value of $S_q(r_i)$ was calculated by averaging a large number of increments of the magnetic field (3×10^5 increments at small r and 1.5×10^5 increments at large r). Therefore, errors in the calculations are very small: they are smaller than the symbol size in Figure 3, where we show results of these calculations for two active regions.

The vertical dashed lines in Figure 3 mark the beginning and the end of the inertial interval, where $\log(S_q(r))$ is a linear function of $\log(r)$ for all q. The structure functions in Figure 3 display the inertial range over one decade of spatial scales. Inertial ranges found for each active region are different, with slightly varying boundaries. The average boundaries for the inertial range, defined for all the active regions, are between 4.0 ± 1 and 25 ± 7 Mm. Having calculated structure functions for different values of q, we are able to calculate function $\zeta(q)$, in accordance with equation (2). This function shows changes in the exponents, as determined inside the inertial interval separations, for each function

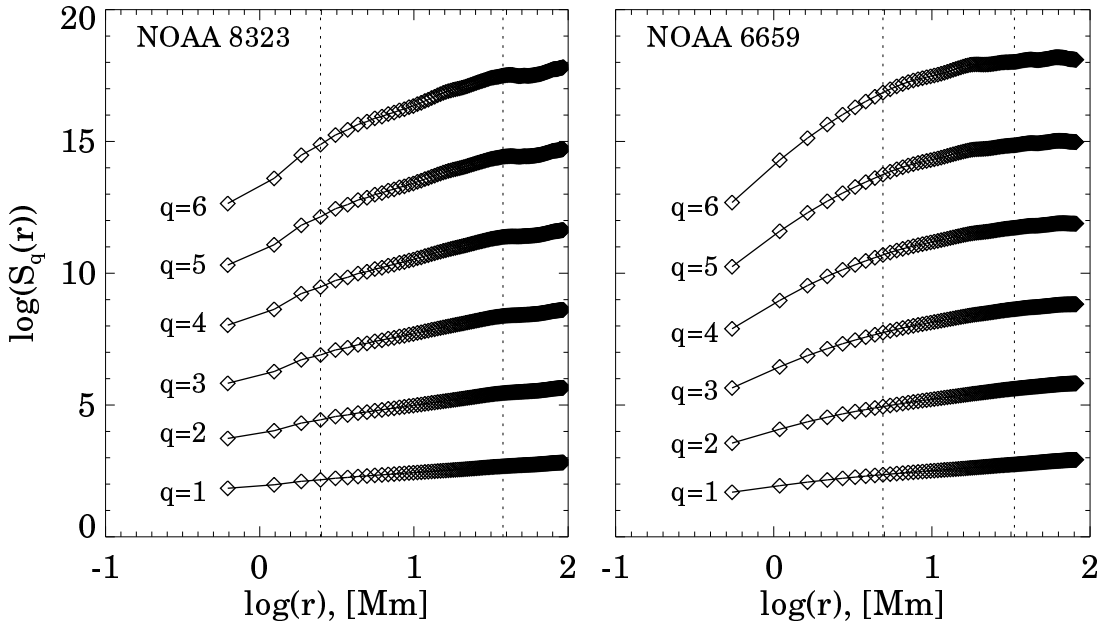

Fig. 3.— A log-log plot of structure functions $S_q(r)$ versus scale r, calculated for the magnetograms presented in Fig. 2. The inertial range separation is shown between the vertical dotted lines.

$\log(S_{q_i}(r))$, versus q_i.

Results of the calculations performed for all active regions are shown in Figure 4. One can see that in all of the cases, the function $\zeta(q)$ deviates from a line with a slope of 1/3 (heretoforward, K41 line), which represents a classical Kolmogorov turbulence.

We would like to draw attention to the fact that in Figure 4 the active regions appear from top to bottom in the same order as they are listed in Tables 1 and 2, namely, in order of increasing flare activity. We estimated each active region's flaring activity using two approaches.

First, in the 2nd column of Table 2, we show the most energetic flare which occurred in each active region prior to the magnetogram acquisition time. For seven active regions these flares also appeared to be the most energetic observed for the entire period of the active region passage across the solar disk.

Second, we estimated the total energy, W, for each active region, released on the day of the observation, by integrating all GOES X-ray flux above B5 level. The total energy, W, reflects the overall activity in an active region and also depends on the solar X-ray emission background.

Table 2: List of active regions, strongest flares in the active regions, X-ray fluxes calculated for the day of observations, W. The X-ray flux is in $10^{-6} Wt \cdot m^{-2} \cdot hour$. The β index is shown in the last column of the table.

NOAA	Flare Class	W	β
8375	M1.0/1N	13.4 ± 1.4	-1.26 ± 0.042
8323	M1.5/1F	5.9 ± 0.6	-1.15 ± 0.064
7216	M1.5/1N	6.5 ± 0.5	-1.02 ± 0.073
7590	M1.8/1B	18.2 ± 1.5	-0.95 ± 0.010
6786	M6.7/2B	37.5 ± 3.1	-0.85 ± 0.034
6757	X1.5/2B	53.7 ± 4.7	-0.60 ± 0.081
6850	M7.4/4B	89.6 ± 10.1	-0.45 ± 0.099
6659	X12/3B	828.0 ± 52.0	-0.27 ± 0.079

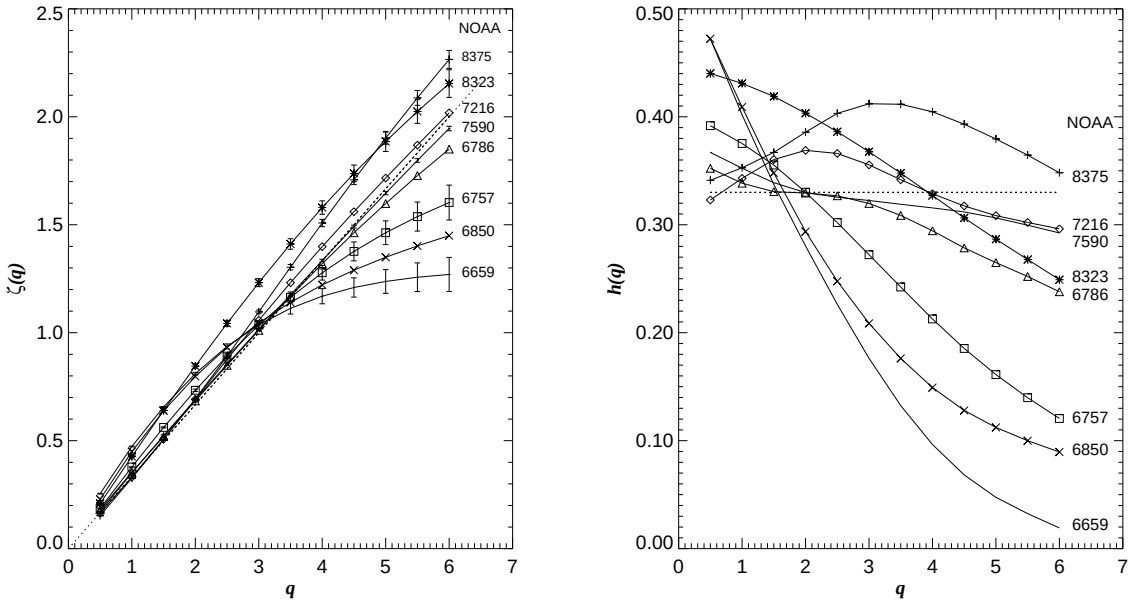

Fig. 4.— Exponents $\zeta(q)$ of structure functions of order q versus q, calculated for eight active regions. The Kolmogorov's straight K41 line with a slope of 1/3 is shown with the dotted line. For the simplicity of the plot, error bars are shown for five active regions only, for the three others they are of the same order.

Fig. 5.— Functions $h(q)$ calculated as derivatives $d\zeta/dq$ for eight active regions. The dotted line shows the Kolmogorov's K41 value for the h. The symbols for each active region are the same as in Fig. 4.

Thus, the active regions in Table 2 are listed in order of increasing activity during the day of the observation, according to the total energy released. The only exception is NOAA

AR 8375, which had a larger parameter W due to higher background emission.

From Table 2 and Figures 4 and 5 we see that for the two active regions with the least flare activity, NOAA AR 8375 and 8323, the function $\zeta(q)$ is always above the K41 line, while in the cases of active regions NOAA AR 7216 and 7590, which showed moderate flare activity, the function $\zeta(q)$ passes very close to the K41 line. For the other four active regions, which produced strong M and X class flares, the $\zeta(q)$ function appears to be much more saturated.

Now we can calculate the derivative, $h(q)$, of the $\zeta(q)$ function according to equation (10). The values $h(q)$, obtained for each active region are shown in Figure 5. All curves deviate from the dotted K41 line. Thus, the B_z-component of the photospheric magnetic field is an intermittent, or a multifractal structure. This conclusion is consistent with the previous result by Lawrence et al. (1993). The degree of intermittency (the interval of allowed h) of the magnetic field in an active region increases as the flaring activity rises.

We shall now consider the scaling of the energy dissipation fields, $\gamma(q)$, which can be calculated based upon equation (11) and the known function $\zeta(q)$. These results are shown in Figure 6. We see that as flaring activity rises, the function $\gamma(q)$ gradually changes from being increasing and positive at all values of q (NOAA AR 8375) to decreasing (at $q > 1.5$) and negative (at $q > 3$).

It is possible to explain this change of characteristics by a competition between the terms $\tau^{(B)}$ and $\tau^{(v)}$ in equation (11), and a gradual transition of a turbulent system with a weakly intermittent magnetic energy dissipation field (case 1, see previous section) to a turbulent system with a highly intermittent magnetic energy dissipation field (case 2, see previous section). Therefore, in active regions with low flaring activity, the B_z-component of the magnetic field behaves as a passive scalar with a weakly intermittent magnetic energy dissipation field and its scaling is mostly determined by the scaling of the kinetic energy dissipation field $\varepsilon_r^{(v)}$. For active regions with high flaring activity the structure functions for the B_z-component behave like transverse structure functions of a 3D turbulent field, and are determined mostly by the magnetic energy dissipation field $\varepsilon_r^{(B)}$.

The most suitable quantitative parameter to describe the above tendency seems to be an index β, defined in (8) and computed by using the known function $\zeta(6)$. As we mentioned earlier, the index β is a power index of a spectrum of energy dissipation of a passive scalar B_z embedded in a turbulent flow. Hereinafter, we will refer to β as an index of B_z-dissipation.

The values of β are presented in the last column of Table 2. The variations in β show that the flatter the spectrum of B_z-dissipation, the higher the flaring activity. This means

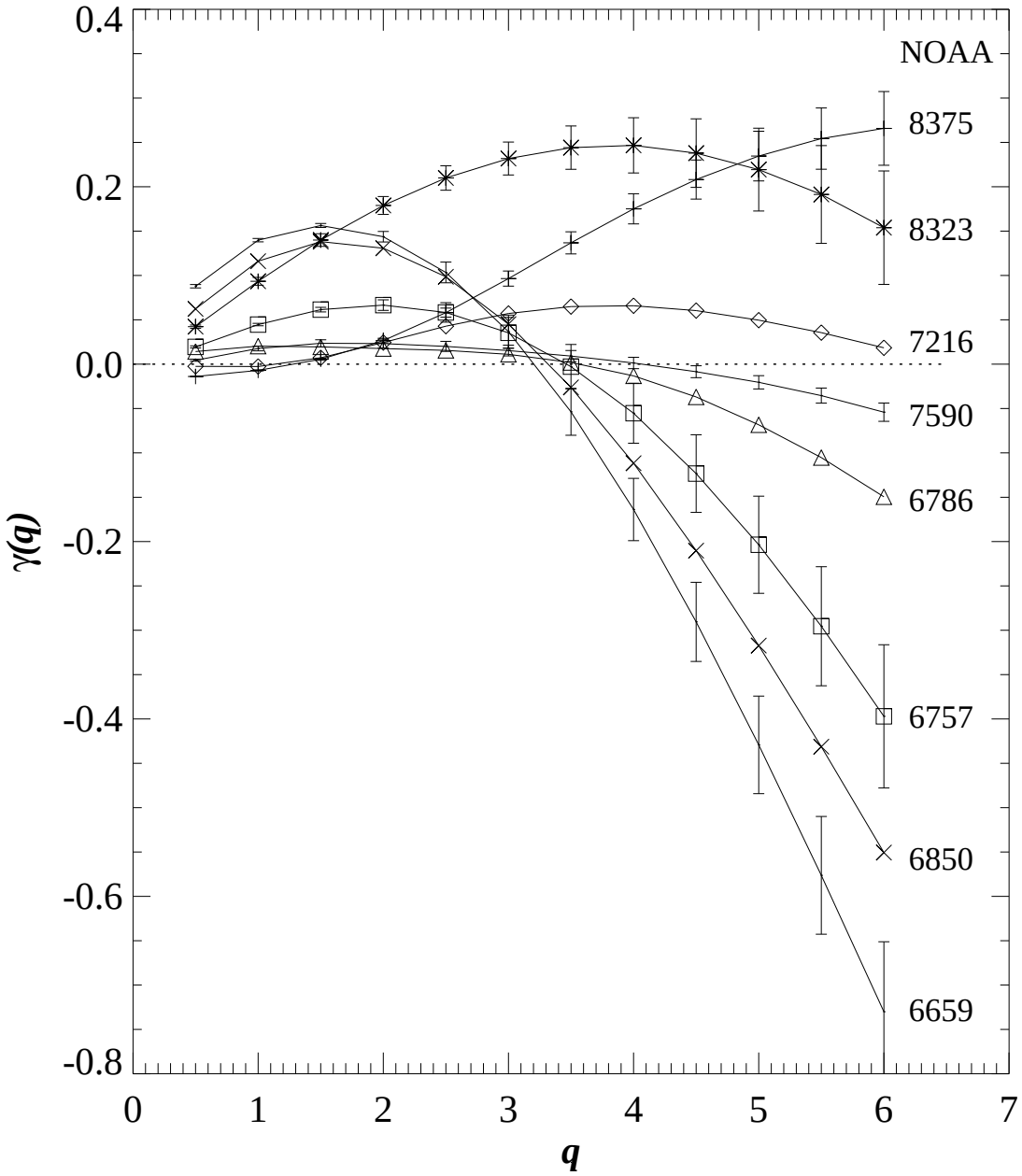

Fig. 6.— Functions $\gamma(q)$ calculated as the deviations of the $\zeta(q)$ from 1/3. The dotted line shows $\gamma(q) = 0$ value for the K41 theory. The symbols for each active region are the same as in Fig. 4.

that the growth of the relative amount of power of magnetic energy fluctuations, at small

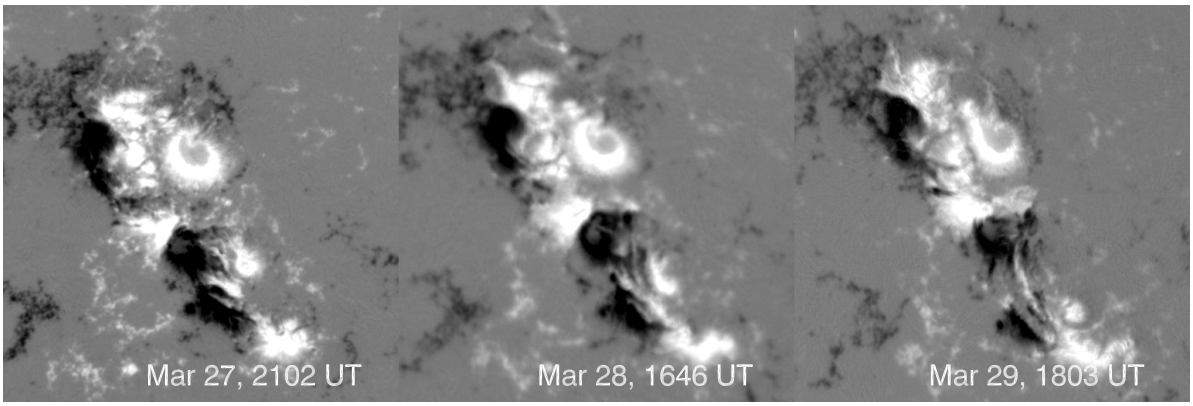

Fig. 7.— BBSO DMG longitudinal magnetograms from March 27–29, 2001.

scales, correlates with rising flare activity. In other words, the stronger the relative role of small-scale fluctuations in the energy dissipation field the more powerful the flare produced.

4. Daily variations of structure functions for the NOAA 9393

The structure functions considered, here for eight active regions, undoubtedly show that the shape of structure functions $\zeta(q)$, and the values of index β of the energy dissipation spectrum, are closely related to the level of flare productivity of a solar active region.

All the aforementioned calculations have been made using one longitudinal magnetogram per day. In order to understand the relation between the longitudinal field changes and flare activity in more detail, we need to study the evolution of an active region over the course of several days.

In Figure 7, we show the Big Bear Solar Observatory Digital Vector Magnetograph (Spirock et al. 2000) measurements of the magnetic field in NOAA AR 9393 on March 27–29, 2001. This sunspot group was one of the most active magnetic regions of solar cycle 23. On March 27–29, 2001 the active region was located near the center of the solar disk (E11 – W13), which allowed us to treat the longitudinal component of the magnetic field as the vertical component, B_z. We used this data to examine the variations of the power index β, and to compare these variations to the corresponding flare activity in the active region.

Figures 8 and 9 show functions $\zeta(q)$ and $\gamma(q)$ on three consecutive days. It is obvious that as the active region evolves both functions become more concave and dive down under the Kolmogorov's K41 line at $q > 4$.

In Table 3 we list the times when the BBSO DVMG longitudinal magnetograms

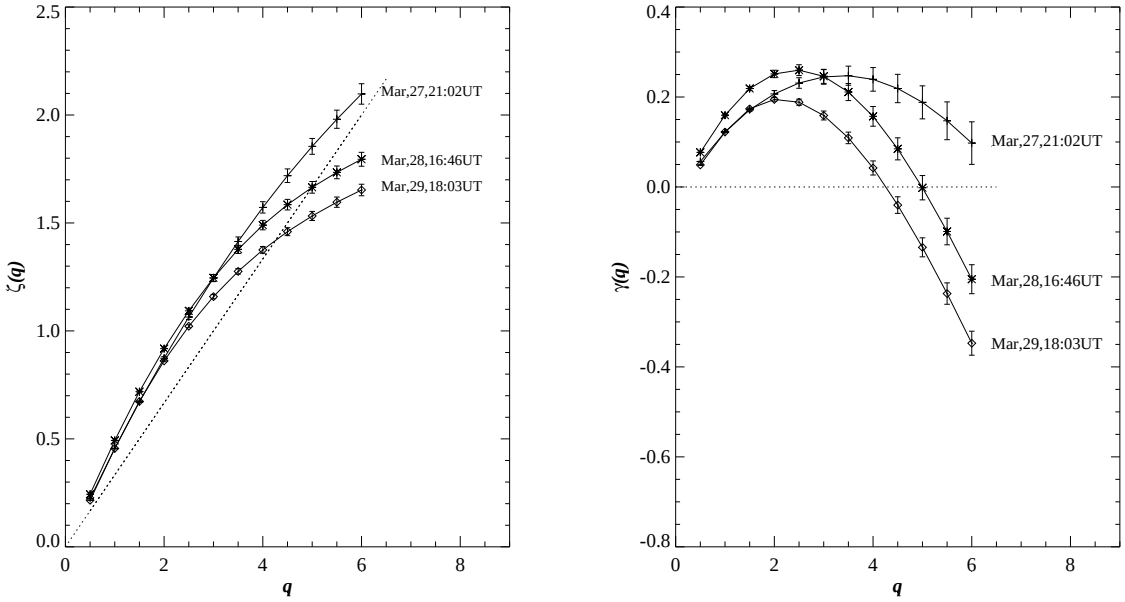

Fig. 8.— Exponents $\zeta(q)$ of structure functions of order q plotted versus q, calculated for three days of observations of NOAA AR 9393. The Kolmogorov's straight K41 line is shown with a dotted line.

Fig. 9.— Functions $\gamma(q)$ calculated as deviations of the $\zeta(q)$ values from 1/3, calculated for three days of observations of NOAA AR 9393. The dotted line shows the $\gamma(q) = 0$ value for the K41 theory.

Table 3: BBSO DVMG observations, the parameter W and the index β. The X-ray flux is in $10^{-6} Wt \cdot m^{-2} \cdot hour$.

Date	Time, UT	W	β
Mar 27, 2001	21:02	73.6 ± 8.1	-1.10 ± 0.047
Mar 28, 2001	16:46	205.7 ± 18.9	-0.80 ± 0.032
Mar 29, 2001	18:03	244.2 ± 15.4	-0.65 ± 0.027

were recorded as well as the parameter W and the index β. It is clear from Table 3 and Figures 8 and 9 that the decrease of β is accompanied by the increase of the parameter W. This behavior is consistent with a transition from a weakly intermittent magnetic energy dissipation field (low flaring activity) to a highly intermittent magnetic energy dissipation field (high flaring activity). On March 27, when the active region produced only C class flares, the parameter β was equal to -1.10. However, the β dropped below -0.8 on March 28 and 29, the days when the active region launched several M and X class flares. As we can see, the index β slowly decreases with time, which indicates the growing probability for

the active region to produce a strong flare. Indeed, on the following two days, the flaring activity rose gradually and the active region had launched additional M and X class flares. Three days later, on April 2, the active region produced the strongest flare observed for the past 25 years.

5. Conclusions

In summary, multifractal properties of the photospheric magnetic field were studied by considering scaling exponents $\zeta(q)$ calculated for increments of the B_z-component of the magnetic field calculated for nine active regions.

The derivative $h(q)$ of function $\zeta(q)$ allowed us to conclude that the B_z-field in an active region is an intermittent (multifractal) structure and the degree of intermittency increases when the flaring activity is rising.

As the level of activity rises the curvature of the function $\zeta(q)$ and its deviation from the K41 line both increases. This allowed us to conclude that when the flaring activity rises, the degree of intermittency of the magnetic energy dissipation field increases and spectrum of the B_z-dissipation becomes more flat (the absolute value of β decreases).

We want to emphasize that the relation between the index β and the flaring activity is not just qualitative. In Figure 10 we plot $\log(|\beta|)$ vs $\log(W)$. The plot demonstrates that there is a linear relation between these two quantities. The asterisks and the diamond represent the HSOS and MDI measurements for 8 active regions (one magnetogram per active region per day), while boxes are the BBSO measurements for NOAA AR 9393 (one magnetogram per day). The solid lines are a linear fit $\log(|\beta|) = A\log(W) + B$ to the HSOS and MDI and to the BBSO data. The plot suggests that for each active region the $\log(|\beta|)$ vs $\log(W)$ relation (the coefficient A) may be close but we may also expect that the $\log(|\beta|) = A\log(W) + B$ line will move along the $\log(W)$ axis depending on the activity level in an active region. In the case of NOAA AR 9393, the larger B value can be caused by the contribution to the total value of W made by a higher number of low C-class flares. The other reason may be that the difference between the instruments and seeing conditions can partially acount for the offset between the fits in Figure 10. However, more data should be analyzed in order to confirm or refute this conclusion.

In order to explain the changes in the $\zeta(q)$ behavior, we used recent analytic results obtained by Abramenko (2002). It has been shown that, assuming that the fluctuations of the energy dissipation of a passive scalar and that of a velocity field are statistically independent, the function $\zeta(q)$ is related to a scaling exponent $\tau^{(B)}$ of the magnetic energy

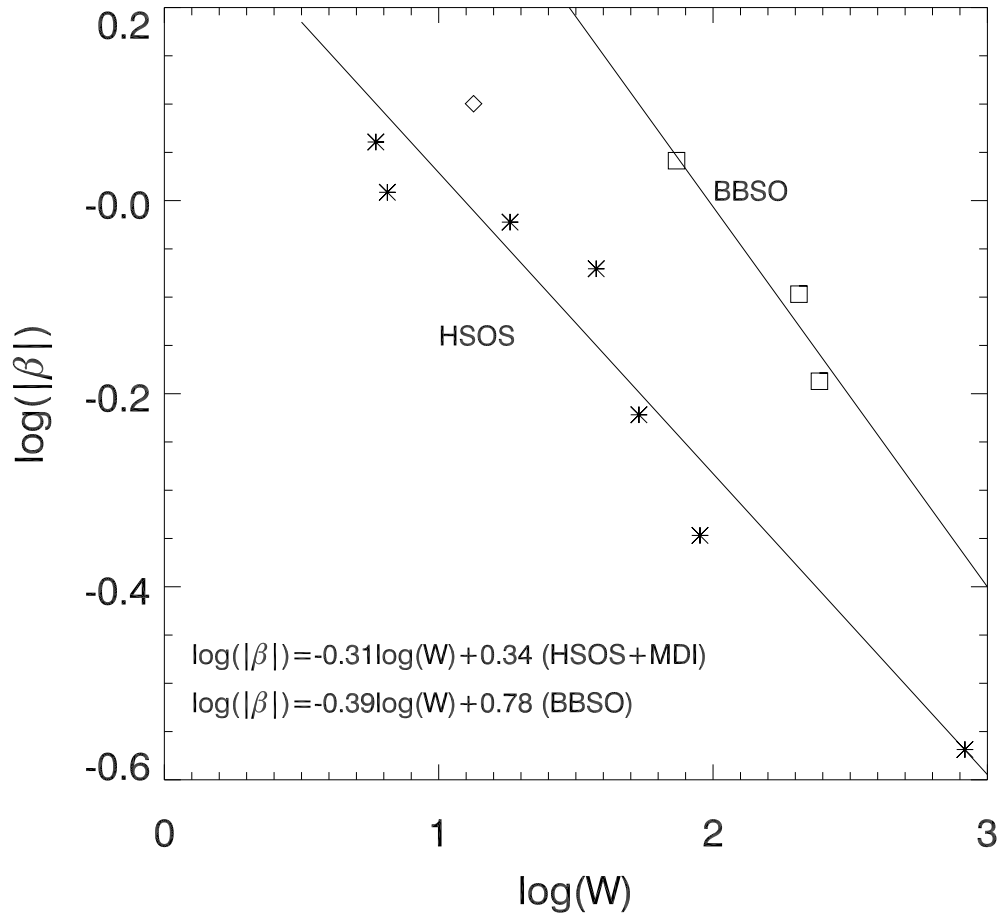

Fig. 10.— Plot of $\log(|\beta|)$ vs $\log(W)$. The asterisks represent the HSOS data and the diamond the MDI measurements for 8 active regions (one magnetogram per active region per day), while boxes are the BBSO measurements for NOAA AR 9393 (one magnetogram per day for three days). The solid lines are linear fit $\log(|\beta|) = A\log(W) + B$ to the HSOS and MDI and the BBSO data separately.

dissipation field $\varepsilon^{(B)}(\mathbf{x})$ (see exp. (11)), as well as with the index β (see exp. (8)) of the B_z-dissipation spectrum. This assumption is based on the fact that the magnetic field is not frozen at the photospheric level. We consider this assumption as a first step toward the understanding of the variety of structure functions observed in active regions. We would also like to emphasize that our main conclusion, that the deviation of the function $\zeta(q)$ from the straight K41 line is due to statistical characteristics of magnetic and kinetic energy dissipation fields, is not affected by the aforementioned assumption. In the case when the assumption does not hold, equation (11) will be more complicated and the theoretical

interpretation of the result would be different. However the conclusion that the shape of the function $\zeta(q)$ is related to the level of flaring activity is still valid.

The conclusion suggests that the relative fraction of *small-scale* fluctuations of magnetic energy dissipation increases as an active region becomes prone to produce strong flares. This supports the idea (Parker, 1987, 1989) that the reorganization of the magnetic field at *small-scales* (not only at large ones) is also relevant to flaring. Moreover, these small scale preflare changes seem to begin long before the start of large scale changes.

The connection between flaring and the magnetic energy dissipation field parameters, suggested in this study, is a natural conclusion since it is the dissipation of magnetic energy that is responsible for flaring in an active region. Direct calculations of $\varepsilon^{(B)}(\mathbf{x})$ require vector magnetic field measurements in some volume with an appropriate sampling not only in the (x, y)-plane, but also in z-direction. Unfortunately, this kind of data is currently unavailable and will more likely remain so in the near future. Therefore, we present here the possibility of using widely available measurements of the B_z-component of the magnetic field to calculate the parameter of the magnetic energy dissipation which may be useful for forecasting flares.

We would like to thank Wang J.X., and Zhang H.Q. for providing the data from HSOS and Kosovichev A. for his help in obtaining the SOHO data. We also thank the anonymous referee for critical comments and suggestions. SOHO is a project of international cooperation between ESA and NASA. This work was supported in part by the Ukrainian Ministry of Science and Education, NSF-ATM (0076602 and 0086999) and NASA (9682 and 9738) grants.

REFERENCES

Abramenko, V.I. 2002, Astron. Reports, 79, N 2, 1

Anselmet, F., Gagne, Y., Hopfinger, E.J., & Antonia, R.A. 1984, J. Fluid Mech., 140, 63

Cadavid, A.C., Lawrence, J.K., & Ruzmaikin, A.A. 1999, ApJ, 521, 844

Cataneo, F. 1999, ApJ, 515, L39

Feder, J. 1988, Fractals (Physics of Solids and Liquids), Plenum Pub. Corp. New York.

Frisch, U. 1995, Turbulence: The Legacy of A.N.Kolmogorov (Cambridge: Cambridge University Press.) 296p.

Gurvich, A.S., & Zubkovsky, S.L. 1963, Bull. Acad. of Sci. USSR, Ser. Geophys., 2, 1856

Kolmogorov, A.N. 1941, C.R. Acad. Sci. USSR, 30, 301

Kolmogorov, A.N. 1962a, Mecanique de la turbulence, Coll. Intern. du CNRS a Marseille. Paris, Ed. CNRS, 447.

Kolmogorov, A.N. 1962b, J. Fluid Mech, 13, 82

Lawrence, J.K., Ruzmaikin, A.A., & Cadavid, A.C. 1993, ApJ, 417, 805

Monin, A.S., & Yaglom, A.M. 1975, Statistical Fluid Mechanics, vol. 2, ed J.Lumley, MIT Press, Cambridge, MA

Parker, E.N. 1979, Cosmical Magnetic Fields. Clarendon Press, Oxford, 841p

Parker, E.N. 1987, Solar Phys., 111, 297

Parker, E.N.:1989, Solar Phys., 121, 271

Petrovay, K., & Szakaly, G. 1993, Astron. Astrophys., 274, 543

Scherrer, P. H., Bogart, R. S., Bush, R. I., Hoeksema, J. T., Kosovichev, A. G., Schou, J., Rosenberg, W., Springer, L., Tarbell, T. D., Title, A., Wolfson, C. J., Zayer, I., & MDI Engineering Team, 1995, Solar Phys., 162, 129

Schmitt, F., Schertzer, D., Lovejoy S., and Brunet Y. 1994, Nonlinear Processes in Geophysics, 1, 95

Seehafer, N. 1994, Astron. Astrophys., 284, 593

Spirock, T. J., Denker, C., Chen, H., Chae, J., Qiu, J., Varsik, J., Wang, H., Goode, P. R., & Marquette, W. 2000, in ASP Conf. Ser. 236, Advanced Solar Polarimetry Theory, Observation, and Instrumentation, ed. M. Sigwarth (San Francisco: ASP), 65

Wang J., Shi Z., Wang H., & Lu Y. 1996, ApJ, 456, 861

Yurchyshyn, V.B., Abramenko, V.I., & Carbone, V. 2000, ApJ, 538, 968

Zeldovich, Ya.B., & Ruzmaikin, A.A. 1987, Uspekhi Fiz. Nauk, 152, Pt. 2, 263